J Mater Sci (2019) 54:10389–10409

Materials for life sciences

Antibacterial activity of sustainable composites derived from epoxidized natural rubber/silver-substituted zeolite/poly(lactic acid) blends

Phruedsaporn Taranamai[1], Pranee Phinyocheep[1,*], Watanalai Panbangred[2], Mayura Janhom[2], and Philippe Daniel[3]

[1] Department of Chemistry, Faculty of Science, Mahidol University, Bangkok 10400, Thailand
[2] Department of Biotechnology and Mahidol University-Osaka, University Collaborative Research Center for Bioscience and Biotechnology (MU-OU: CRC), Faculty of Science, Mahidol University, Bangkok, Thailand
[3] Institut des Molécules et des Matériaux du Mans (IMMM) UMR CNRS 6283, Le Mans Université, Av. O. Messiaen, 72085 Le Mans Cedex 9, France

Received: 22 December 2018
Accepted: 4 April 2019
Published online: 10 April 2019

© Springer Science+Business Media, LLC, part of Springer Nature 2019

ABSTRACT

Sustainable composites derived from epoxidized natural rubber (ENR)/silver-substituted zeolite (AgZ)/poly(lactic acid) (PLA) blends possessing antibacterial activity were reported. ENR, herein, acted as an antibacterial promoter providing more hydrophilicity to the composites and facilitating water diffusion. Two methodologies were used to prepare composites, including solution casting (S) as well as solution casting followed by roll milling (SR). Both composites were compared in terms of morphology, AgZ dispersion, water absorption, and antibacterial activity. The shift of T_g and tan δ toward lower temperature of PLA composites consistently confirmed the compatibility between ENR and PLA by DSC and DMA results, respectively. The good AgZ distribution was observed in composites-SR, as confirmed by SEM/EDX. The results of agar disk diffusion susceptibility test showed that PLA, AgZ/PLA, and even ENR/AgZ/PLA composites-S showed no or less inhibition zone; meanwhile, ENR/AgZ/PLA composites-SR showed the significant inhibition zone against both *Escherichia coli* and *Staphylococcus aureus*. Besides, the antibacterial activity of the composites was required at least 5 wt% of AgZ. More than 98% inhibition of *S. aureus* growth by the composites-SR was observed during 2–24 h of cultivation, whereas AgZ/PLA provided the highest inhibition of only 75% at 24 h of cultivation. Hence, the incorporation of ENR enhances the bactericidal activity of the composites. In terms of mechanical properties, incorporating ENR into the composites decreased tensile modulus and strength, but increased the impact strength significantly. Therefore, the developed composites could be promising materials in food and biomedical fields in which antibacterial and impact resistance properties are required.

Address correspondence to E-mail: pranee.phi@mahidol.ac.th

https://doi.org/10.1007/s10853-019-03599-1

Introduction

The development of antibacterial thermoplastics has gained more attention from industrial and academic sectors since these functional materials might be a solution for microbial contamination [1–6]. Poly(lactic acid) (PLA), nowadays, becomes the most useful bio-based thermoplastic because of its interesting properties, including biodegradability, biocompatibility, renewability, and good mechanical properties. It has been widely used in commercial and biomedical applications, e.g., plastic packaging and containers. Hence, the development and functionalization of PLA products having antibacterial activity are of great importance.

Among antibacterial agents, silver-substituted zeolites (AgZ) have been applied in various applications [5–16] because the silver ions released from the zeolite framework are effective against a broad range of bacterial strains [17, 18]. When AgZ was mixed with polymers, the migration of silver ions to the surface of material is a crucial factor to exhibit the antibacterial activity. The release of active substances from polymeric materials could be explained using swelling-controlled model [19, 20]. It is proposed that water penetrates into the matrix of polymer to allow swelling of the polymer network and then carries the active substances to the surface of polymer for inhibiting bacterial growth. For this reason, the molecular diffusion of active substance is dependent on the characteristic of polymer, as flexible polymer facilitates more transportation compared to glassy polymer [21].

PLA is, literally, a semi-crystalline polymer with hydrophobicity in its nature. The poor water absorption characteristic and low diffusivity of small molecules in PLA matrix limit the use of PLA-based materials in antibacterial applications. Ahmed et al. [22] studied the antibacterial effectiveness of PLA/poly(ethylene glycol), (PEG) film containing silver–copper alloy nanoparticles (NP). They found that all composites films had no effectiveness against tested bacteria because no zone of inhibitions could be observed. On the other hand, Fernandez et al. [23] reported the antibacterial activity of AgZ/PLA composites against *E. coli* and *S. aureus*. But only slight decrease in the number of bacterial colonies was observed, despite the fact that the antibacterial susceptibility test was performed in minimal medium which poorly supports the bacterial growth. According to these publications, the hydrophobicity of PLA is the cause of poor antibacterial activity.

We hypothesized that blending PLA with the second polymer having high polarity and flexibility to promote the diffusion of active substances in the PLA network might help in releasing Ag ions. Moreover, the selected second polymer must be bio-based and environmentally friendly polymer to produce sustainable antibacterial composites. Epoxidized natural rubber (ENR) which is a modified form of natural rubber is a choice of interest because of its properties. Up to now, the number of ENR/PLA blends as well as clay/ENR/PLA composites were prepared and the improved mechanical properties, toughness in particular, of PLA were reported [24–28]. However, the fabrication of these blends having antibacterial activity has never been found. On that account, this work will broaden the utilization of ENR/PLA composites in the applications in which both impact resistance and antibacterial activity are of great importance.

In this study, Ag in the form of AgZ was mixed with either PLA or ENR/PLA composites and their antibacterial activity was compared. The preparation and characteristic of the targeted composites prepared by different methods were discussed. The distribution of AgZ in the composites and the water absorption behaviors were investigated. Besides, we have demonstrated that blending the hydrophobic PLA with hydrophilic ENR allowed the efficient release of Ag and could improve the antibacterial activity as shown by the reduction of bacterial growth (*S. aureus*) more than 98% during 2–24 h of cultivation. Hence, this study will pave the way toward the multifunctional ENR/PLA containing AgZ that can be used in high-value added applications, e.g., coating, plastic containers or packaging for food and medical industries.

Experimental

Materials

Poly(lactic acid) pellets (2003D) were purchased from Natureworks. Zeolite 4A (ADVORA®401) was kindly supported by PQ Chemical (Thailand) Co., Ltd. Silver-substituted zeolites were prepared according to the ion-exchange process as reported elsewhere [29] and the amount of silver ions in zeolite was 4.6% as

confirmed by EDX detector. High ammonia natural rubber latex was purchased from Thai Rubber Latex Corporation (Thailand) Public Co., Ltd. Formic acid was purchased from Merck. Hydrogen peroxide was purchased from Fluka. Tergitol (15-S-15) was purchased from Dow Chemical Thailand Ltd. Mueller–Hinton broth was purchased from Merck. Agar granule was the product by Difco. *E. coli* (ATCC25922) and *S. aureus* (ATCC25923) were used as indicator strains for antibacterial susceptibility test.

Preparation of zeolites (Z) or silver-substituted zeolites (AgZ)/PLA composites

Firstly, PLA pellets, Z, and AgZ were dried in a conventional oven at 100 °C for 2 h. After that, either Z or AgZ was pre-mixed with PLA pellets in plastic bags. To prepare composites, the pre-mixed materials were then fed into a hopper of a twin-screw extruder (TSE) (Prism TSE16, Staffordshire, UK). The temperatures in feeding, barrel, and die zones were 150 °C, 180 °C, and 180 °C, respectively. The screw speed was 80 rpm. The obtained product was cut into small pieces and then dried in an oven at 80 °C overnight. After that, the product was kept in a desiccator to avoid moisture absorption.

Preparation of epoxidized natural rubber

60 ml of Natural rubber latex (NR latex) with 20% dry rubber content (DRC) was firstly stabilized with 5 phr non-ionic surfactant (Tergitol). The stabilized NR latex was heated to 60 °C. Then, 0.5 mol of formic acid and 2 mol of hydrogen peroxide, which were calculated compared to the isoprenic units of NR, were added simultaneously into the stabilized NR latex for generating in situ performic acid. The reaction mixture was stirred for 24 h. At the end of the reaction, the reaction mixture was precipitated in methanol and then the obtained product was dried in a vacuum oven at room temperature until the weight was constant. After that, the obtained ENR was masticated at room temperature using a two-roll mill (Pornviwat Engineering, laboratory two-roll mill model 10) for 5 min with 0.5 mm nip gap.

Preparation of ENR/PLA blends and ENR/AgZ/PLA composites

ENR/PLA blends were prepared by solution blending. The desired amount of PLA pellets and masticated ENR were separately dissolved in 400 ml of dichloromethane. After that, the ENR solution was poured into the PLA solution and the solution mixture was then stirred overnight to obtain a homogeneous solution. At the end of the solution blending process, the solution mixture was poured onto a glass plate and the obtained sample was dried at 50 °C overnight.

In the case of ENR/AgZ/PLA composites, the desired amount of PLA pellets and masticated ENR were separately dissolved in 400 ml of dichloromethane. After that, the ENR solution was poured into the PLA solution and the solution mixture was stirred for 5 min. before adding various amounts of AgZ (1 wt%, 3 wt%, and 5 wt%). The solution mixture was then stirred overnight to obtain a homogeneous solution. At the end of the solution blending process, the solution mixture was poured onto a glass plate and the obtained sample was dried at 50 °C overnight.

The obtained ENR/AgZ/PLA composites were classified into two categories based mainly on the preparing methodologies, which were solution casting (S) and solution casting together with roll milling (SR). The composites prepared by the solution casting and solution casting together with roll milling were abbreviated as composites-S and composites-SR, respectively. For composites-S, after the solvent evaporation, the obtained sample was cut into small pieces and then shaped into a sheet using a compression molding at 170 °C for 2 min. In the case of composites-SR, after the solvent evaporation the obtained sample was milled using a two-roll mill at room temperature for 5 min with 0.5 mm nip gap to increase the dispersion of AgZ in the composites. Then, the composites-SR were cut into small pieces and then shaped by means of a compression molding at 170 °C for 2 min. All samples were kept in a desiccator to avoid moisture absorption. Table 1 shows the ingredients of all samples used in this study.

Structural characterization

^{1}H-NMR spectroscopy was applied to analyze the chemical structure of ENR. About 10 mg of sample

was dissolved in deuterated chloroform ($CDCl_3$) containing tetramethyl silane (TMS) as an internal reference. The ^{1}H-NMR spectrum was recorded on Bruker AM 400 spectroscopy 500 MHz. The degree of epoxidation (%E) was determined using following equation.

$$\%E = \frac{A_{2.7}}{A_{2.7} + A_{5.1}} \times 100 \quad (1)$$

where $A_{2.7}$ and $A_{5.1}$ were the integrated area of protons adjacent to oxirane ring and double bond of NR, respectively. In this work, the epoxidation degree was found to be 45%.

Molecular weight determination

The molecular weight of ENR and masticated ENR was determined by gel permeation chromatography (GPC) (Water 150-CV). At first, the sample was dissolved in THF. All sample solutions were filtered with 0.22 μm syringe filter nylon (PA) membrane before analysis. The flow rate of THF eluent was at 1 ml/min at 40 °C using a guard column (Polymer Laboratories, Styragel @HR 5E, 7.8 × 300 mm) including an RI detector with PS standard. The number average molecular weight ($\bar{M}_n$), weight average molecular weight ($\bar{M}_w$), and polydispersity index (PDI) of the samples were recorded.

Thermal behavior of composites

The thermal behavior of composites was characterized using differential scanning calorimeter (DSC TA Q200). The specimen was scanned from 40 to 200 °C at the heating rate of 20 °C/min. Next, the specimen was cooled down from 200 to 40 °C at the cooling rate of 20 °C/min. After that, the temperature was increased to 200 °C with the heating rate of 20 °C/min. Glass transition temperature (T_g), cold crystallization temperature (T_{cc}), and melting temperature (T_m) were recorded.

Dynamic mechanical analysis

Dynamic mechanical properties of samples were examined by using dynamic mechanical analyzer (GABO EPLEXOR 25N) under the temperature sweep test at frequency of 5 Hz under static and dynamic strains of 1 and 0.1%, respectively. The testing temperature was scanned in the range of − 80 °C to 80 °C at heating rate of 2 °C/min. Storage (E') and loss (E'') moduli and damping factor (tan δ) of samples were investigated.

Morphology of composites

Before investigating the morphology of the composites, the specimens of ENR/AgZ/PLA composites were immersed in xylene for 4 h to remove the ENR phase. After that, all samples were submerged in liquid nitrogen and cryogenically fractured to expose

Table 1 Ingredients of composites used in this study

Sample	Processing method	Compositions (%)			
		PLA	ENR	Z or AgZ	Ag
PLA	–	100	–	–	–
5ZPLA	Melt mixing	95	–	5	–
5AgZ/PLA		95	–	5	0.2
10ENR/PLA-S	Solution casting	90	10	–	–
20ENR/PLA-S		80	20	–	–
30ENR/PLA-S		70	30	–	–
10ENR/5AgZ/PLA-S		90	10	5	0.2
20ENR/5AgZ/PLA-S		80	20	5	0.2
30ENR/5AgZ/PLA-S		70	30	5	0.2
20ENR/1AgZ/PLA-SR	Solution casting and roll milling	80	20	1	0.05
20ENR/3AgZ/PLA-SR		80	20	3	0.1
10ENR/5AgZ/PLA-SR		90	10	5	0.2
20ENR/5AgZ/PLA-SR		80	20	5	0.2
30ENR/5AgZ/PLA-SR		70	30	5	0.2

to the internal structure of the blends. After that, all of the samples were sputtered with Pt/Pd. The morphologies of the composites in two different sides which were the fracture surface and outer surface were investigated using scanning electron microscope (SU-8010, Hitachi) at an acceleration voltage of 10 kV. The droplet size of ENR was measured and then at least fifty particles were used to calculate the average particle size.

The distribution of zeolites in composites-S and composites-SR was also compared by energy-dispersive X-ray spectroscopy (EDX, equipped in scanning electron microscope (SU-8010, Hitachi).

Water absorption of composites

All samples were shaped into a sheet with thickness of 1 mm. The prepared samples were pre-conditioned by drying in an oven at 50 °C overnight. After that, the samples were immersed into a well-controlled water bath (SPC group, digital heat) at 37 ± 1 °C. Water immersion testing, herein, was carried out in agreement with ASTM D570. The water absorption test was performed until reaching the equilibrium and weight changing of samples was recorded after periodic removal of the samples from the water bath. The surface of specimens was dried using tissue papers before recording the weight by means of a weighting balance (AND/Japan model G-200). The experiment was repeated three times. The percentage of water absorption at any time t (M_t) caused by the moisture absorption was determined by Eq. 2.

$$M_t(\%) = \frac{W_w - W_d}{W_w} \times 100\% \quad (2)$$

where W_d and W_w denote weight of dry specimen (the initial weight of PLA specimens prior to being immersed into water) and weight of PLA specimens after being exposed to water. Additionally, the percentage at equilibrium or maximum water absorption (M_m) was calculated as the average value from several consecutive measurements showing no significant absorption.

Antibacterial activity of composites

The inhibition activity of composites was carried out by placing the specimens (square sheet with 1 mm × 1 mm × 0.4 mm) on agar plates seeded with *E. coli* or *S. aureus* (the initial concentration of both strains was 10^6 cfu/ml). Then, the agar plates were incubated at 37 °C. The inhibition zone was evaluated by measuring the width of the inhibition zone at 24 h after incubation using a digital caliper. The actual inhibition zone was calculated by subtraction the width of specimens. The experiment was repeated five times.

Besides, the plate count technique was also used to evaluate the antibacterial efficacy of the composites. *S. aureus* was pre-cultured and inoculated in 50 ml of Mueller–Hinton (MH) broth to obtain the OD value of 0.1. The plastic sheets (5 × 5 cm^2) were placed in flasks containing 50 ml Mueller–Hinton broth loaded with the bacterial solution with OD value of 0.1. The flasks were incubated in a reciprocal shaker at a shaking speed of 100 rpm at 37 °C for 24 h. At time interval, 0, 2, 4, 6, 12, 18, and 24 h, 100 µL of each sample was taken and a tenfold serial dilution was performed for bacterial colony counting. Serial diluted solution (100 µL) was spread on MH agar plate and incubated at 37 °C for 24 h. The bacteria colonies were counted to assess the antibacterial activity of the composites. The antibacterial activity of the composites was expressed in terms of log number of colony forming units per milliliter (log cfu/ml), and the experiment was repeated twice. Moreover, the reduction percentage of bacterial colonies was calculated by using Eq. 3.

$$\%\,\text{Reduction} = \frac{A - B}{A} \times 100\% \quad (3)$$

where A is the average number of bacterial colonies from culture broth containing neat PLA for a given contact time (cfu/ml), and B is the average number of bacterial colonies from culture broth containing either AgZ/PLA or ENR/AgZ/PLA-SR for a given contact time (cfu/ml).

Mechanical properties

For investigating mechanical properties of the composites, all samples were shaped using a compression molding at 170 °C. For tensile testing, the samples were shaped into a sheet with 0.4 mm in thickness. The tensile properties were tested using a tensile testing machine (Instron 5566) in agreement with ASTM D882. The average value of at least five specimens of tensile strength, modulus, and elongation at break was reported.

The notched Izod impact strength of PLA and its composites was also investigated. The testing sample with 3 mm in thickness was prepared. Notched Izod impact strength was measured using a Zwick impact tester according to ASTM D256. At least, 5 specimens were used and the average results of testing were reported in the unit of KJ/m^2.

Results and discussion

Preparation of epoxidized natural rubber (ENR)

The methodology to prepare ENR corresponded with our previous publication [30]. Briefly, the desired amount of hydrogen peroxide and formic acid are simultaneously added into the stabilized NR latex to generate in situ performic acid which further reacts with isoprenic units of NR. Figure 1 exhibits the ^{1}H-NMR spectra of NR and ENR. The proton H_a referred to the proton adjacent to double bond of isoprenic units was found at 5.1 ppm. After epoxidation reaction, the new signal (H_b) at 2.7 ppm, which was the characteristic signal of the proton adjacent to epoxide ring, was clearly observed. The degree of epoxidation can be calculated (Eq. 1) by comparing the integration area of the methine proton adjacent to the oxirane ring at 2.7 ppm and that of the proton adjacent

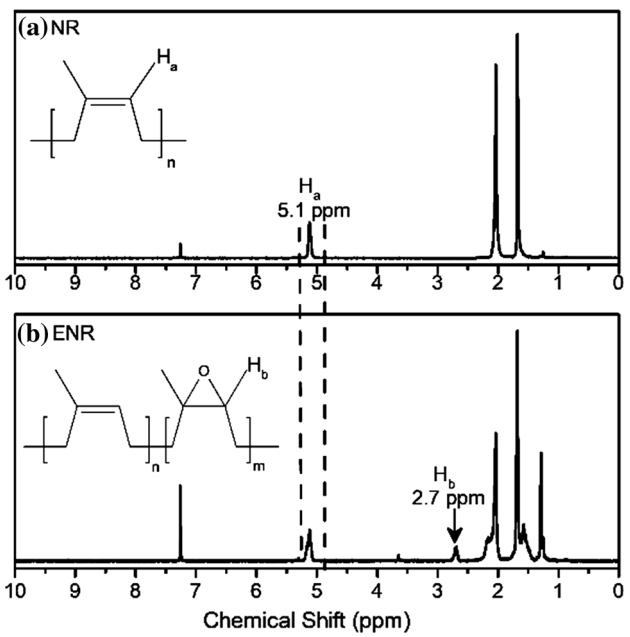

Figure 1 ^{1}H-NMR spectra of **a** NR and **b** ENR.

to the carbon–carbon double bond of isoprenic units at 5.1 ppm [30–33]. The degree of epoxidation of ENR was found to be 45%.

The obtained ENR was masticated by means of a two-roll mill to reduce molecular weight of the rubber in order to improve the solubility of ENR in dichloromethane. The $\bar{M}_n$ and $\bar{M}_w$ of ENR before mastication process were 427,000 g/mol, and 1,159,000 g/mol, respectively. After the mastication process, the molecular weight of ENR was remarkably reduced. The $\bar{M}_n$ and $\bar{M}_w$ of masticated ENR were 185,200 g/mol and 341,000 g/mol, respectively. The decrease in molecular weight of ENR by the mastication process is attributed to the shear force which mechanically breaks down the rubber chains [27].

Thermal behaviors and compatibility of composites

As previously mentioned, ENR/AgZ/PLA composites prepared in this work can be classified into two categories, which were composites-S and composites-SR, corresponded with the preparing methodologies. The solution blending is, generally, considered as a useful method to prepare a polymer blend. Nevertheless, when inorganic fillers were mixed with polymer blends, some parts of inorganic fillers may sediment at the bottom part of the samples during the solvent evaporation process because of the particle–particle interaction [34]. This phenomenon leads to non-homogeneity of the obtained composites. Hence, in this work, roll milling together with solution blending was carried out to investigate the blends with improved homogeneity.

Thermal behaviors of neat PLA, 5Z/PLA, 5AgZ/PLA and ENR/AgZ/PLA composites-S and composites-SR were investigated as shown in Fig. 2. Figure 2a shows the second heating scan of all composites. DSC thermograms of neat PLA and 5Z/PLA showed the cold crystallization and melting peaks. In the case of 5AgZ/PLA, the decrease in the cold crystallization and melting peaks was observed. This might be due to silver ions hindering the crystallization of the composites. For ENR/AgZ/PLA composites, it can be clearly seen that there were no traces of crystallization occurred for both composites-S and composites-SR, which was due to the high compatibility between ENR and PLA that interfered the crystallization process of PLA [24]. The thermal

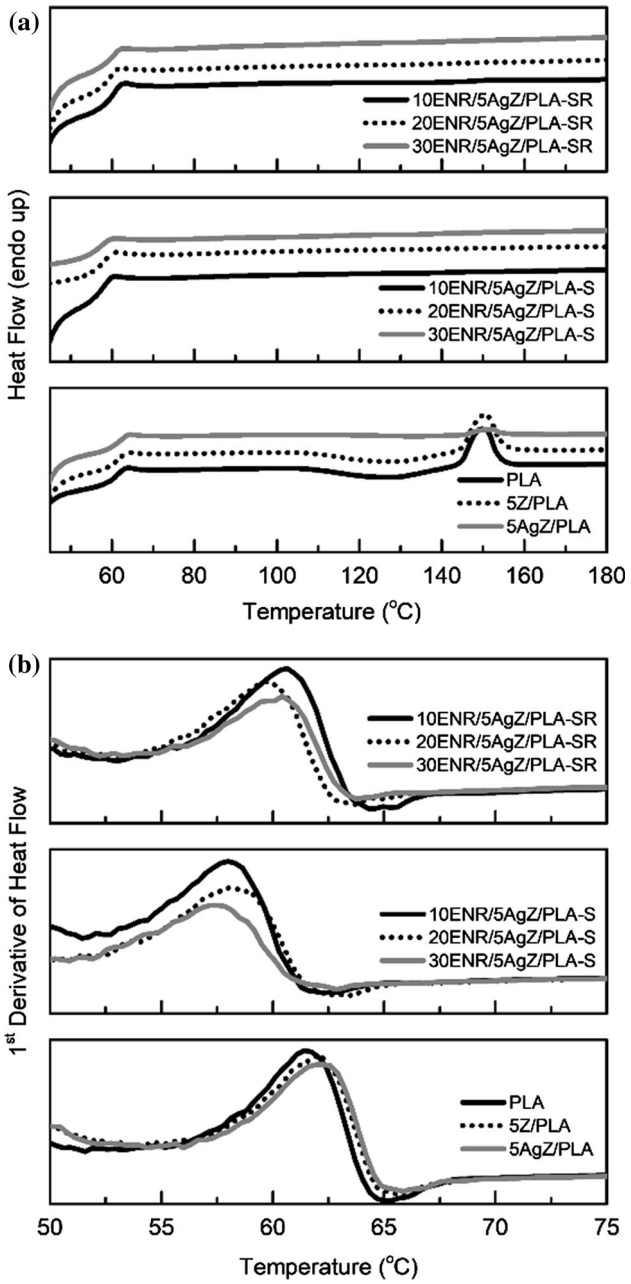

Figure 2 Thermal characterization of the composites; **a** DSC thermograms of neat PLA and the composites, and **b** their first derivatives of heat flow in the range of 50–75 °C.

properties of neat PLA and PLA composites are shown in Table 2.

To further investigate the change of T_g of PLA in the composites, the first derivative of heat flow in the range of 50–75 °C was carried out. Figure 2b shows the first derivative of the second heating scan of all composites which clearly indicated the change of T_g after incorporating Z, AgZ, and ENR. The Tg values of PLA, 5Z/PLA, and 5AgZ/PLA were 61.4 °C, 62.0 °C, and 62.0 °C, respectively. In the case of ENR/AgZ/PLA composites, the shift of T_g of PLA toward lower temperature was observed because of the compatibility between ENR and PLA caused by the oxirane ring of ENR and carbonyl group of PLA [24]. In the composites-S, the T_g values of 10ENR/5AgZ/PLA-S and 20ENR/5AgZ/PLA-S were decreased to 58.0 °C. Increasing the content of ENR in the composites-S to 30 wt% slightly lowered the T_g of PLA to 57.3 °C. This is due to the increase in the amount of oxirane ring that can interact with carbonyl group of PLA.

In the case of composites-SR, it was unanticipated that after the roll milling process the T_g values of the composites-SR were higher than those of the composite-S containing the same amounts of ENR and AgZ. The detail of this phenomenon is further scrutinized via dynamic mechanical analysis, as follows.

Dynamic mechanical analysis was used to investigate the compatibility and the interaction of ENR, PLA, and AgZ in the composites-S and composites-SR. The binary blend of ENR/PLA and the ternary blend of ENR/AgZ/PLA having ENR content equal to 20% were selected as representative samples to study the effect of the roll milling process on the dynamic mechanical properties of the composites. The storage modulus of the composites as a function of temperature is exhibited in Fig. 3. The results showed that at the temperature below − 50 °C, the storage modulus of ENR/PLA and ENR/AgZ/PLA composites were similar, because both ENR and PLA are in the glassy state. In the range of − 50 °C to 50 °C (as shown in Fig. 3b), the storage modulus of PLA remained constant, while the storage moduli of 20ENR/PLA, 20ENR/5AgZ/PLA-S, and 20ENR/5AgZ/PLA-SR dropped significantly since ENR becomes rubbery. The results showed that the storage modulus of 20ENR/5AgZ/PLA-S was higher than that of 20ENR/PLA because the applied stress can be transferred to the zeolites particles leading to the increase in the storage modulus of the composites [35]. Nonetheless, the storage modulus of 20ENR/5AgZ/PLA-SR was lower than that of 20ENR/5AgZ/PLA-S in spite of the fact that these two samples contained the same amount of AgZ. It could be hypothesized that the roll milling process led to the better distribution of the zeolites. Besides, in the range of 55–80 °C (Fig. 3c), the significant decrease in the storage modulus of neat PLA, ENR/PLA blend,

Table 2 Results of T_g, T_{cc}, T_m, ΔH_f, and χ_c of PLA and various PLA composites

Sample	T_g (°C)	T_{cc} (°C)	T_m (°C)	ΔH_f (J/g)	χ_c (%)
PLA	61.4	127.7	149.9	8.37	2.0
5Z/PLA	62.0	128.5	150.3	8.20	1.4
5AgZ/PLA	62.0	133.6	151.3	0.24	0.3
10ENR/5AgZ/PLA-S	58.0	–	–	–	–
20ENR/5AgZ/PLA-S	58.0	–	–	–	–
30ENR/5AgZ/PLA-S	57.3	–	–	–	–
10ENR/5AgZ/PLA-SR	60.6	–	–	–	–
20ENR/5AgZ/PLA-SR	59.7	–	–	–	–
30ENR/5AgZ/PLA-SR	60.3	–	–	–	–

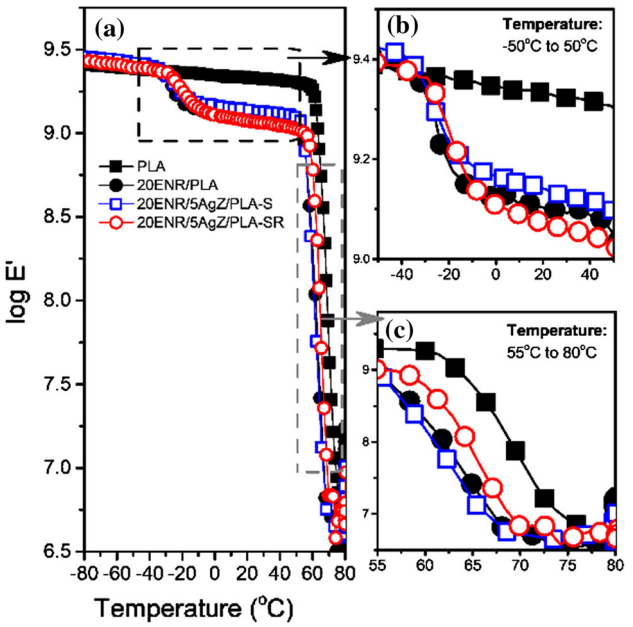

Figure 3 Storage modulus of PLA, 20ENR/PLA, 20ENR/5AgZ/PLA-S, and 20ENR/5AgZ/PLA-SR.

and ENR/AgZ/PLA composites could be observed because the temperature is in the rubbery region of PLA. It can be clearly seen that the dramatic decrease in the storage modulus of the samples in this region occurred at different temperature. To further investigate the detail of this phenomenon, the tan δ results of these composites were discussed in the following details.

Tan δ of neat PLA, ENR/PLA, ENR/AgZ/PLA composites-S, and ENR/AgZ/PLA composites-SR were investigated as shown in Fig. 4. It can be clearly seen that neat PLA showed only one peak at 70 °C. On the other hand, ENR/PLA, 20ENR/5AgZ/PLA-S, and 20ENR/5AgZ/PLA-SR showed two tan δ peaks in which the tan δ peak at low temperature (− 40 °C to 0 °C, as shown in the inset) referred to the tan δ peak of ENR and the tan δ peak at high temperature (50–80 °C, as shown in the inset) belonged to the tan δ peak of PLA.

Considering the low temperature region, the tan δ of ENR in 20ENR/PLA was observed at − 23 °C, while the tan δ of 20ENR/5AgZ/PLA-S shifted toward lower temperature. After the roll milling process, the tan δ value of 20ENR/5AgZ/PLA-SR shifted toward higher temperature, but the value of tan δ was still the same. For this reason, it could be postulated that there was the interaction between ENR and zeolites; thus, higher temperature was required to cause the movement of ENR chains. To get better understanding about this phenomenon, the inset illustrating the tan δ in the region of 50–80 °C must be taken into consideration. The results showed

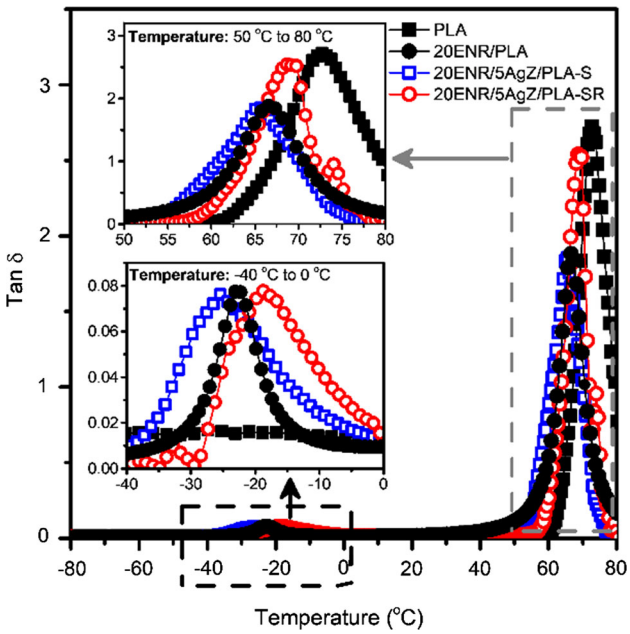

Figure 4 Tan δ of PLA, 20ENR/PLA, 20ENR/5AgZ/PLA-S, and 20ENR/5AgZ/PLA-SR.

that blending PLA with 20 wt% ENR significantly decreased the value of tan δ because of the dilution effect caused by ENR content. For 20ENR/5AgZ/PLA-S, the tan δ value and the peak position were close to the tan δ peak of 20ENR/PLA. On the other hand, the tan δ of 20ENR/5AgZ/PLA-SR was noticeably different from the tan δ of 20ENR/5AgZ/PLA-S, as the tan δ shifted toward higher temperature and the value of tan δ increased significantly. The shift of tan δ, herein, was corresponded with the shift of T_g toward higher temperature obtained by DSC. It could be hypothesized that the roll milling process resulted in better dispersion of the zeolite in composites-SR than composites-S; hence, some parts of zeolites residing formerly in the PLA phase might move to the interphase between ENR and PLA. Therefore, zeolites could interact better with ENR, leading to the decrease in the influence of rubber on the energy loss during the glass state to rubber transition of PLA.

Morphology of composites

The morphologies of neat PLA and the composites were investigated as shown in Fig. 5a–h. The SEM image of PLA showed the smooth surface. For 5AgZ/PLA, the result showed the dispersion of AgZ in the PLA matrix. Although, some zeolite particles were still embedded in the matrix which was due to the interfacial interaction between zeolites and PLA [35], the aggregation of zeolite particles and voids around the zeolites which were referred to the incompatibility of PLA and zeolites could still be observed. The average particle size of zeolites was about 2.00 μm. After incorporating ENR into the composites, the morphology of composites-S was completely different compared to that of PLA and 5AgZ/PLA, the sea-island morphology in which the ENR particles distributed in the matrix of PLA was observed for all ENR/5AgZ/PLA-S. Increasing the ENR content in the composites led to the enlargement of ENR droplets caused by the coalescence of ENR phase. The sizes of ENR particles of 10ENR/5AgZ/PLA-S, 20ENR/5AgZ/PLA-S and 30ENR/5AgZ/PLA-S were 2.01 μm, 2.32 μm, and 4.51 μm, respectively. Additionally, it can be seen that the zeolite particles were distributed in PLA and ENR phases and less voids were observed compared to 5AgZ/PLA composites because the oxirane ring of ENR interacted with both hydroxyl groups of zeolites and PLA leading to the good compatibility in the composites [24]. The details about the morphologies of composites are shown in Table 3.

For the composites-SR, the SEM images of 10ENR/5AgZ/PLA-SR and 20ENR/5AgZ/PLA-SR exhibited the sea-island morphology which was the same as the composites-S at the same ratio. The sizes of ENR phase in 10ENR/5AgZ/PLA-SR and 20ENR/5AgZ/PLA-SR were 2.06 μm and 2.29 μm, respectively. In 10ENR/5AgZ/PLA-SR composites, some zeolite particles were still embedded in the matrix of PLA. Meanwhile, the morphology of 20ENR/5AgZ/PLA-SR was slightly different from that of 10ENR/5AgZ/PLA-SR as the elongated phase of ENR could be seen. Furthermore, the location of zeolites was dissimilar with that of zeolites found in 20ENR/5AgZ/PLA-S since the result illustrated that some of zeolites aggregated and resided at the location at which ENR phase appeared or between the interphase of ENR and PLA. For 30ENR/5AgZ/PLA-SR, the morphology of the composites was changed from the sea-island morphology to co-continuous morphology in which the elongated ENR phase continuously distributed in the PLA matrix as shown in Fig. 5h. Additionally, the zeolites particles were located at the interphase of ENR and PLA.

Figure 6 shows the surface of the composites after etching by xylene. For the composites-S, the morphology of the composites containing different amount of ENR was similar and the location of zeolites (the arrows pointed out the location of zeolites) was consistent with that observed in Fig. 5 (zeolites embedded in PLA phase). Interestingly, the SEM images of composites-SR could be noticed differently in terms of both morphology and zeolite location compared to the composites-S. In 10ENR/5AgZ/PLA-SR, some zeolites could be found at the surface of specimen. Furthermore, increasing the amount of ENR to 20 wt% and 30 wt% exhibited a bunch of zeolites on the surface of 20ENR/5AgZ/PLA-SR and 30ENR/5AgZ/PLA-SR. In this experiment, during the etching process, xylene plays a role to dissolve the ENR phase from the composites. It could be implied that if most of zeolites residing at the interphase between ENR and PLA, the solvent extraction might cause the migration of zeolites to the surface of specimens. On the other hand, if most of zeolites staying in PLA phase, the solvent extraction would not cause the delocalization of zeolites because xylene cannot dissolve PLA at room temperature. It

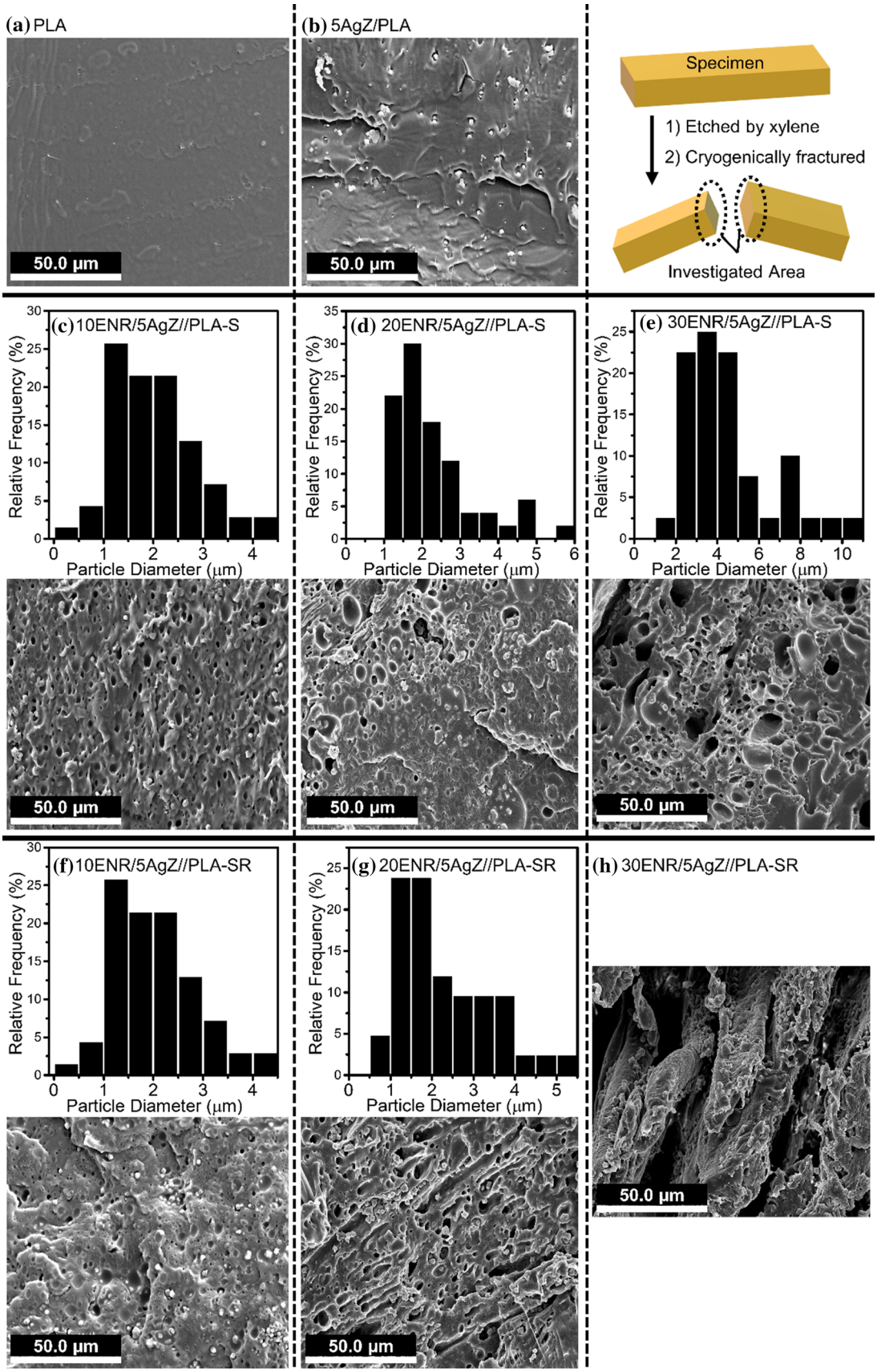
(a) PLA
50.0 μm
(b) 5AgZ/PLA
50.0 μm
Specimen
1) Etched by xylene
2) Cryogenically fractured
Investigated Area
(c) 10ENR/5AgZ//PLA-S
Relative Frequency (%)
Particle Diameter (μm)
50.0 μm
(d) 20ENR/5AgZ//PLA-S
Relative Frequency (%)
Particle Diameter (μm)
50.0 μm
(e) 30ENR/5AgZ//PLA-S
Relative Frequency (%)
Particle Diameter (μm)
50.0 μm
(f) 10ENR/5AgZ//PLA-SR
Relative Frequency (%)
Particle Diameter (μm)
50.0 μm
(g) 20ENR/5AgZ//PLA-SR
Relative Frequency (%)
Particle Diameter (μm)
50.0 μm
(h) 30ENR/5AgZ//PLA-SR
50.0 μm

◀**Figure 5** SEM images of fractured surfaces of **a** PLA, **b** 5AgZ/PLA, **c** 10ENR/5AgZ/PLA-S, **d** 20ENR/5AgZ/PLA-S, **e** 30ENR/5AgZ/PLA-S, **f** 10ENR/5AgZ/PLA-SR, **g** 20ENR/5AgZ/PLA-SR, and **h** 30ENR/5AgZ/PLA-SR.

Table 3 Type of morphology and size of ENR particles in the composites

Sample	Morphology	ENR particle size (μm)
PLA	Smooth	–
5Z/PLA		–
10ENR/5AgZ/PLA-S	Sea-island	2.01 ± 0.87
20ENR/5AgZ/PLA-S		2.32 ± 1.07
30ENR/5AgZ/PLA-S		4.51 ± 2.10
10ENR/5AgZ/PLA-SR	Sea-island	2.06 ± 0.82
20ENR/5AgZ/PLA-SR		2.29 ± 1.09
30ENR/5AgZ/PLA-SR	Co-continuous	–

could be therefore concluded that the roll milling process not only elongates the ENR phase, but also alters the location of zeolites which could be confirmed by SEM, DSC and DMA results, as displayed in Fig. 7.

Besides, the distribution of zeolites in the composites was also investigated using energy-dispersive X-ray (EDX) spectroscopy, as shown in Fig. 8. The fractured surfaces of composites-S and composites-SR with the ENR content of 20 wt% were used to study the discrepancy of zeolite distribution. Aluminum (Al) and silicon (Si) atoms which correspond to the main structural compositions of zeolites were used to evaluate the distribution of zeolites in these composites. From Al- and Si-mapping, the well-distributed zeolite particles were found in the EDX mapping of composites-SR.

Water absorption

The study of water absorption characteristic of polymer is of great importance for antibacterial thermoplastics, because the active ingredients used to kill bacteria are required to diffuse to the surface of polymer materials via water intermedia [19, 20]. The water absorption behavior of composites-S and composites-SR are therefore investigated, and their results are displayed in Fig. 9. It can be clearly seen that the water absorption curves of all composites were increased at the beginning and then leveled off when reaching equilibrium. The percentage at equilibrium or maximum water absorption (M_m) value of PLA equals to 0.89%, meaning that only small

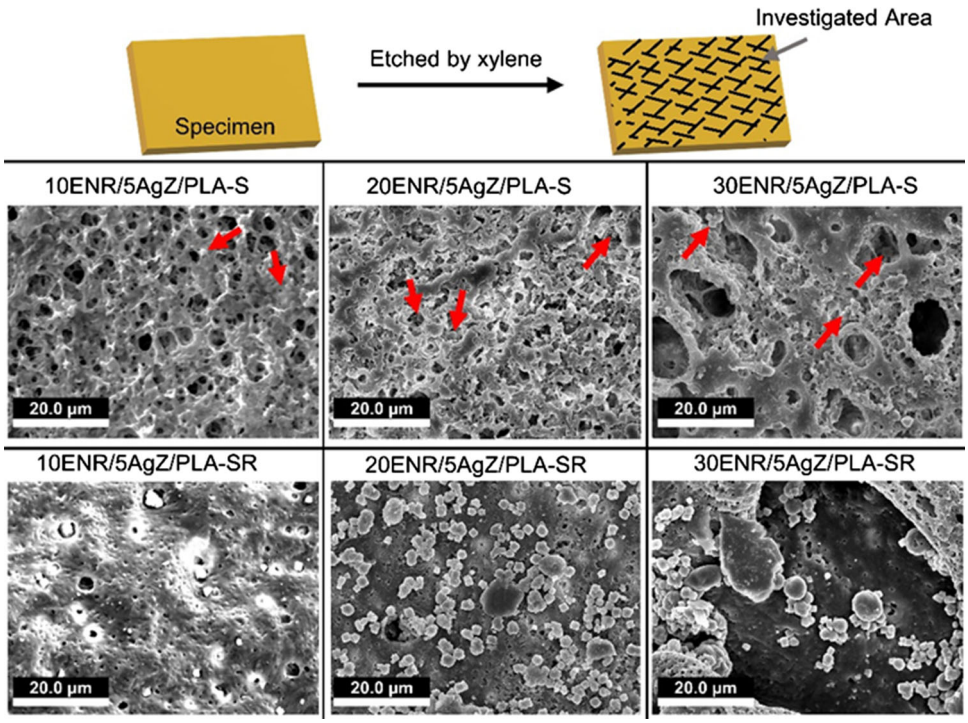

Figure 6 SEM images of surfaces of composites-S and composites-SR after etching by xylene.

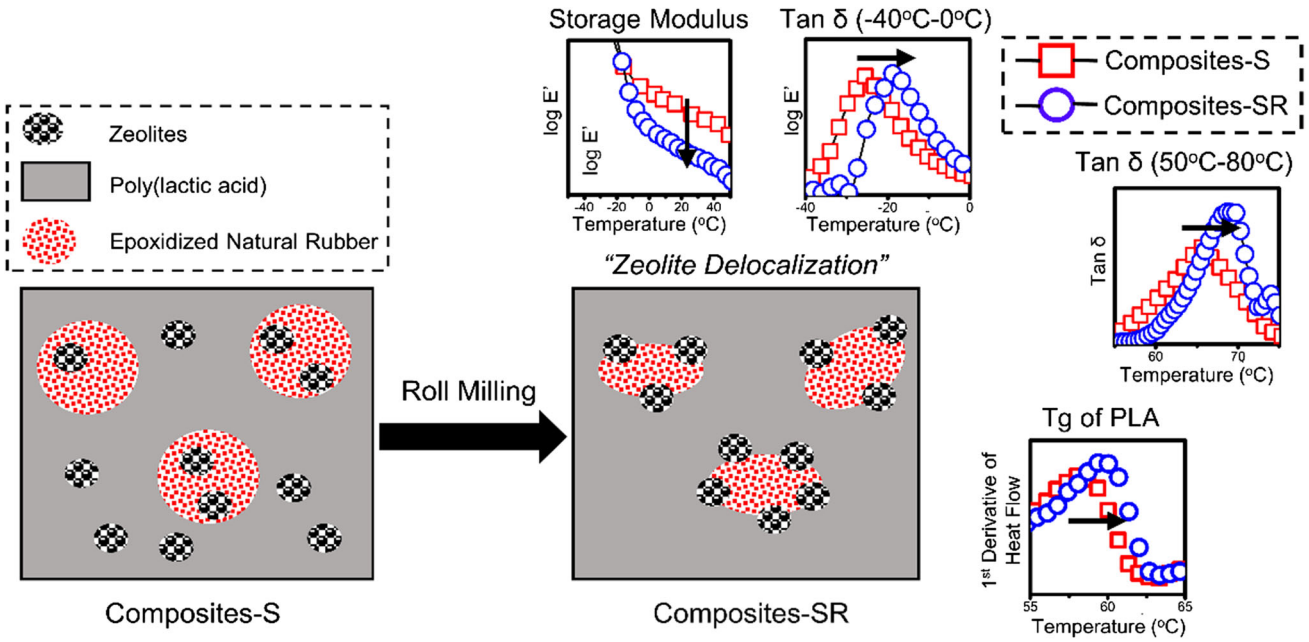

Figure 7 Schematic illustration of the delocalization of zeolites in the composites.

amount of water molecules could penetrate into the PLA matrix because of its hydrophobicity [36, 37]. After blending PLA with 5 wt% of zeolites, the M_m value of the composites increased remarkably from 0.89 to 1.47%. The increase in the M_m of the composites was attributed to the hydroxyl groups of zeolites which are available to interact with water molecules [35].

In the case of ENR/AgZ/PLA composites, the incorporation of ENR into the composites exhibited the increase in the M_m values in composites-S and composites-SR (as shown in Fig. 9a–c) because of the hydrophilicity of epoxide groups on the rubber chains. The presence of polar groups, which tend to interact with water molecules, in the polymer composites leads to the increase in the water uptake and thus facilitates the water diffusion in the composites [28, 38]. The M_m values of 10ENR/5AgZ/PLA-S, 20ENR/5AgZ/PLA-S, and 30ENR/5AgZ/PLA-S were 2.11, 2.36, and 3.20%, respectively. It could be noted that the significant increase in the M_m value was observed with further increasing ENR content, which was due to the increase in the amounts of hydrophilic groups that can interact with water molecules. For composites-SR, the maximum water absorption percentages of 10ENR/5AgZ/PLA-SR and 20ENR/5AgZ/PLA-SR were close to composites-S at the same ratios. Meanwhile, the M_m value of 30ENR/5AgZ/PLA-SR reached 5.54% which was noticeably higher than the M_m of composites-S having the same rubber content. The explanation might be due to the morphological difference between these composites. The 30ENR/5AgZ/PLA-SR possessed the co-continuous morphology with the larger ENR phase size in comparison with 30ENR/5AgZ/PLA-S (shown in Figs. 5, 6), leading to the increase in the void content of the composites. Hence, the water uptake of the composites increased since the maximum water absorption percentage is dependent on the void content [39]. Kushwaha et al. [40] studied the water absorption characteristic of untreated- and treated bamboo/polyester composites. It was found that the maximum water uptake of untreated- and treated bamboo/polyester composites was 51% and 35%, respectively. The disparity of the water uptake was attributed to the poor wettability and the adhesion between untreated bamboo and matrix leading to the void formation.

According to above results, it could be concluded that the increase in the ENR contents favors the penetration of water molecules into the composites leading to the increase in the maximum water absorption percentage. The morphology of ENR phase also plays a role in the water uptake of composites. The increment of water absorption will cause the change in antibacterial performance of PLA composites, as discussed in the following details.

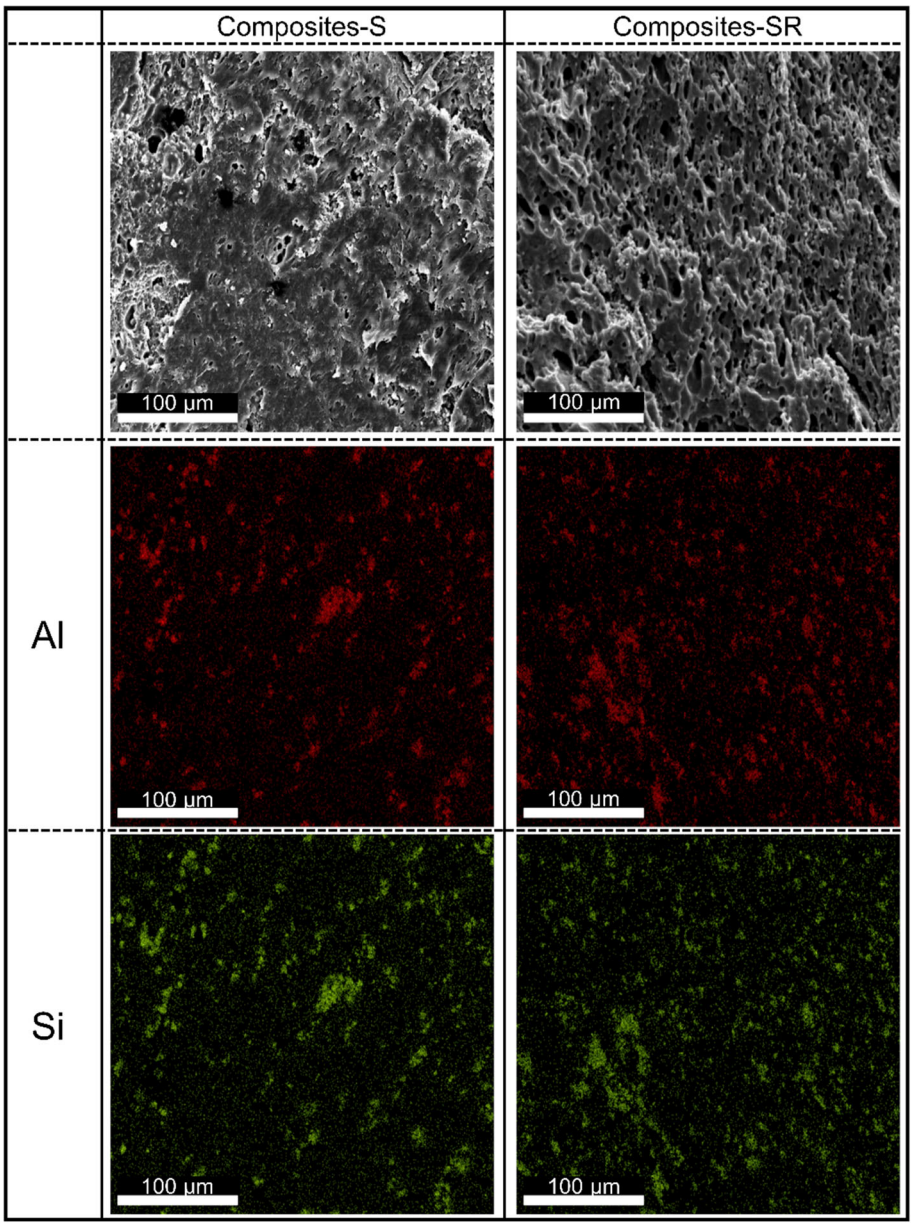

Figure 8 SEM-EDX of composites-S and composites-SR with the same AgZ (5 wt%) and ENR (20 wt%) contents.

Antibacterial activity of composites

To evaluate the antibacterial performances of the composites, both qualitative and quantitative analyses were carried out, including agar disk diffusion susceptibility test and total viable plate count technique.

Agar disk diffusion susceptibility test

At first, ENR and the binary blends of ENR/PLA containing different amount of ENR (10–30 wt%) were tested against *E. coli* and *S. aureus*, as shown in Fig. 10. ENR and ENR/PLA binary blends did not exhibit the antibacterial activity since there was no inhibition zone generated by the tested samples. Hence, it could be noted that ENR itself could not inhibit the growth of bacteria.

Figure 11a shows the inhibitory of various composite sheets which were tested against *E. coli* and *S. aureus*. PLA exhibited no zone of inhibition, meaning that PLA did not possess the antibacterial activity against these two strains. Also, 5AgZ/PLA composites showed no zone of inhibition despite the fact that it contains AgZ in the PLA. The reason might be due to the hydrophobicity of PLA, which allowed only

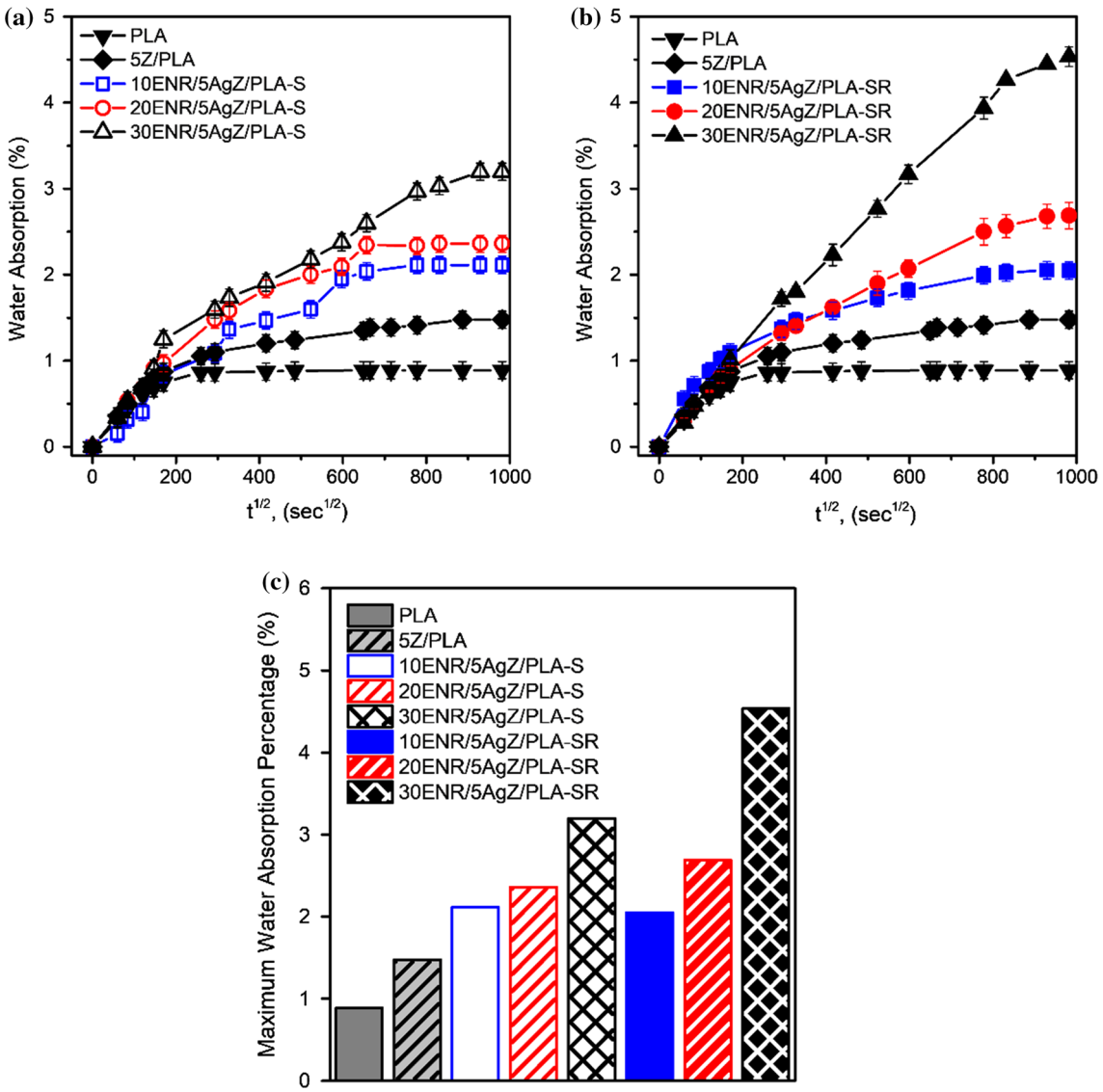

Figure 9 Plots of water absorption percentage as a function of time of **a** PLA, 5Z/PLA, and ENR/AgZ/PLA composite-S, **b** PLA, 5Z/PLA, and ENR/AgZ/PLA composites-SR, and **c** the maximum water absorption percentage of PLA, 5Z/PLA, ENR/AgZ/PLA composites-S, and ENR/AgZ/PLA composites-SR.

limited amount of silver ions to be migrated to the surface of specimens leading to the unsatisfactory antibacterial activity [22]. Nevertheless, the antibacterial activity of silver-substituted zeolites/PLA composites was reported in another publication [23]. However, only the slight decrease in the log reduction of viable colonies about 1.02 (for *E. coli*) and 0.8 (for *S. aureus*) was reported after 24 h of incubation.

ENR, herein, plays a role to improve the antibacterial activity of PLA composites because the polarity and the flexibility of ENR facilitate the diffusion of water molecules in the composites. For composites-S, 10ENR/5AgZ/PLA-S, 20ENR/5AgZ/PLA-S, and 30ENR/5AgZ/PLA-S (as shown in Fig. 11a, b, disks III, IV, V) exhibited no or very small inhibition zone at only one or two side of specimen (Fig. 11b, disks IV and V). The reason behind the antibacterial ineffectiveness of the composites-S was attributed to the sedimentation of AgZ caused by the particle–particle interaction during the solution blending step. Hence, even the sample was cut into small pieces before being shaped into the sheets, the antibacterial activity of the composites-S was still insufficient.

According to the antibacterial results of composites-S, it could be noted that the antibacterial activity of PLA composites seemed to be improved by mixing

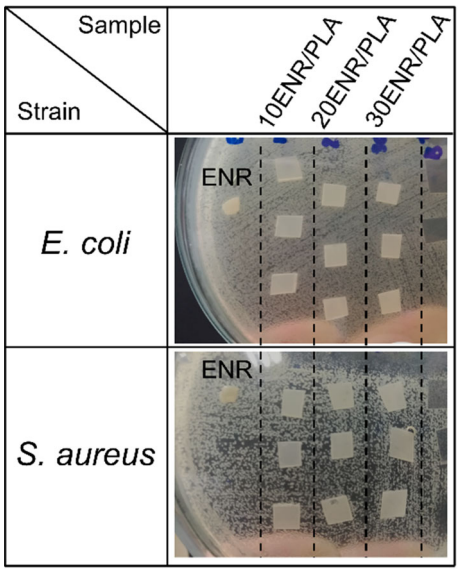

Figure 10 Antibacterial tests of ENR, 10ENR/PLA, 20ENR/PLA, and 30ENR/PLA against *E. coli* and *S. aureus*.

with ENR because the inhibition zones could be found in some specimens. Nevertheless, the poor distribution of AgZ in the composites still occurred. Hence, the homogeneity of the composites-S should be enhanced. As mentioned above, the roll milling was selected to improve the homogeneity of the composites, as stated by the other publication that this process was useful to enhance the homogeneity of fillers in the thermoplastics [41]. As shown in Fig. 11a, b, the antibacterial results showed that all of composites-SR exhibited the inhibition zone around the specimens. The inhibition zones created by the composites-SR were symmetric, meaning that the distribution of AgZ in the composites-SR was much better than that of composites-S. The inhibition zones of the composites-SR are listed in Table 4. The inhibition zones of 10ENR/5AgZ/PLA-SR, 20ENR/5AgZ/PLA-SR, and 30ENR/5AgZ/PLA-SR against *E. coli* were 0.25, 0.95, and 0.25 mm, respectively. According to the results, it could be noted that increasing the amount of ENR in the composites from 10 to 20 wt% led to the increase in the inhibition zone which was due to the enhancement of flexibility and polarity facilitating the migration of silver ions to the surface of the specimen, as supported by the water absorption experiment shown earlier. Meanwhile, the inhibition zone of 30ENR/5AgZ/PLA-SR was lower than that of 20ENR/5AgZ/PLA-SR, which might be due to the fact that the surface area of the co-continuous morphology in 30ENR/5AgZ/PLA-SR was

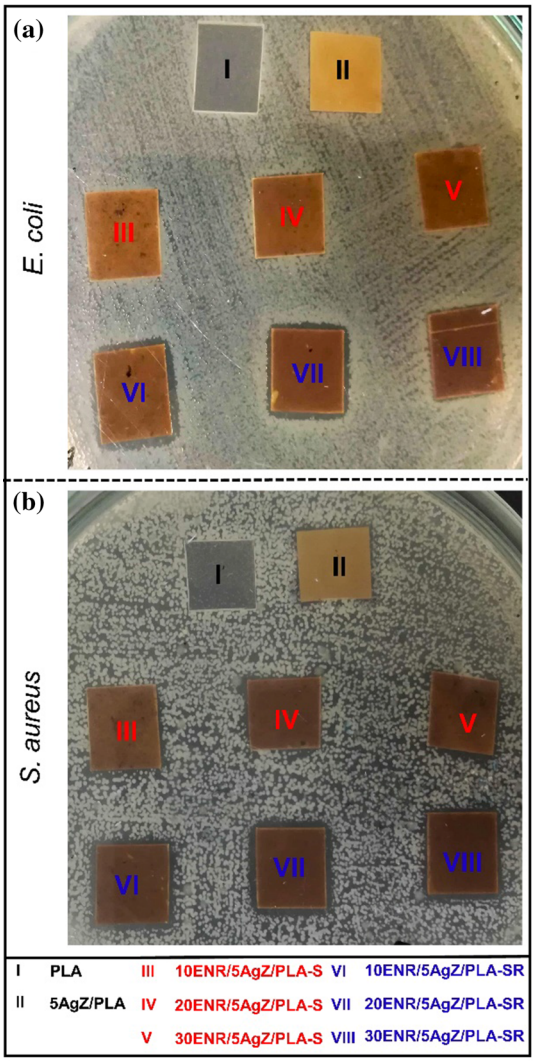

Figure 11 Agar disk susceptibility tests of neat PLA, AgZ/PLA, and ENR/AgZ/PLA composites tested against **a** *E. coli* and **b** *S. aureus*.

lower than that of the sea-island morphology in 20ENR/5AgZ/PLA-SR.

The antibacterial activity of the composites-SR against *S. aureus* showed that only 10 wt% of ENR was satisfactory to express the inhibition zone of 3.23 mm. Increasing the amount of ENR in the composites to 20 wt% led to the slight increase in the inhibition zone. Nevertheless, the higher amount of ENR in the composites showed the decrease in the inhibition zone which was similar with the test of *E. coli*. From these results, it could be noted that the composites-SR were far more effective against *S. aureus* as reflected by the larger inhibition zone. The reason is due to the gram-positive bacteria (such as, *S. aureus*) have a thicker peptidoglycan layer which

Table 4 Zone of inhibition of composites-SR containing different amount of ENR against *E. coli* and *S. aureus*

Sample	Inhibition zone (mm)	
	E. coli	*S. aureus*
Neat PLA	–	–
5AgZ/PLA	–	–
10ENR/5AgZ/PLA-SR	0.25	3.23
20ENR/5AgZ/PLA-SR	0.95	3.70
30ENR/5AgZ/PLA-SR	0.30	3.40
20ENR/1AgZ/PLA-SR	–	–
20ENR/3AgZ/PLA-SR	–	1.47

–, no inhibition zone

would attract higher amount of silver ions leading to the death of bacterial cells [42–46].

The amount of AgZ in the composites-SR was also varied in the range of 1–5 wt% to study the influence of the amount of AgZ on the antibacterial activity of the composites, and the results are given in Table 4. In the case of 1 wt% AgZ in the composites, there was no inhibition zone against *E. coli* and *S. aureus* observed, suggesting that the amount of AgZ in the composites was not sufficient to inhibit the growth of bacteria. Meanwhile, 20ENR/3AgZ/PLA-SR possessed the inhibition zone against *S. aureus* (1.47 mm), but could not inhibit the growth of *E. coli*. The reason is due to the fact that gram-positive bacteria is more susceptible to silver ions than gram-negative bacteria, as previously mentioned. Consequently, it could be noted that at least 5 wt% of AgZ is needed to exhibit the antibacterial activity against *E. coli* and *S. aureus*.

Inhibition of *S. aureus* growth by PLA, 5AgZ/PLA and 20ENR/5AgZ/PLA-SR

To quantitatively evaluate the antibacterial performance of PLA and PLA composites, the total viable count was applied. PLA was used as a control. To highlight the point in which ENR acts as an antibacterial promoter of AgZ/PLA composites, the silver-substituted zeolites/PLA composites with- and without ENR were compared and *S. aureus* was selected as a model. The living bacteria colonies in terms of log (cfu/ml) and the reduction percentage of bacteria at different contact times are given in Fig. 12. It was observed that for neat PLA the number of living cells increased when the contact time increased, suggesting that neat PLA does not have the ability to delay or inhibit the growth of bacterium. In the case of 5AgZ/PLA, *S. aureus* still continued to grow when the incubating time increased, but the total cell count was lower than that of neat PLA. The percentage of bacterial reduction during 12 h of the culture was in the range of 30–40% (Fig. 12b). After that, the significant increase in the reduction percentage was exhibited, which was due to the fact that the higher amount of silver ions was released from the composites at the longer contact time. For 20ENR/5AgZ/PLA-SR composites, it was found that the number of living bacterial cells was rapidly reduced for 2–5 log values during 2–12 h (Fig. 12a). However, the bacterial growth increased again at 18 and 24 h of cultivation. The percentage of bacteria reduction confirmed the high antibacterial efficiency of the composites-SR since the reduction percentage reached 98% at the very beginning of the experiment and steadily stayed (98–99%) until 24 h. The highest percentage of bacteria reduction of AgZ/PLA was 75% at 24 h. The explanation for the greater antibacterial activity of the composites-SR compared to AgZ/PLA was due to the fact that ENR, which is flexible and hydrophilic polymer, increased the water absorption of the composites (as confirmed by the water absorption experiment discussed earlier), leading to the higher amount of silver ions migrating to the broth. Another publication reporting a hydrophilic substance to promote the antibacterial activity of PLA was the work done by Prapruddivongs and Sombatsompop [47]. The authors used wood flour to enhance the antibacterial performance of triclosan/PLA by facilitating the migration of silver ions. The improvement of the antibacterial activity was found in the sample containing wood flour. However, the antibacterial experiment was tested in peptone solution which is the poor medium and the contact time was only 4 h. Besides, the antibacterial activity observed in our work was far more effective compared to another publication that used AgZ/PLA composites [23]. They reported that only slight decrease in the number of living bacterial cells occurred after 24 h of incubation in a diluted TSB/water (1:125) medium, which is also a poor medium.

Furthermore, the physical appearance of the broth being contacted with the composites-SR was clear compared to the opaque broth of PLA and AgZ/PLA indicating high cell density in the latter cases

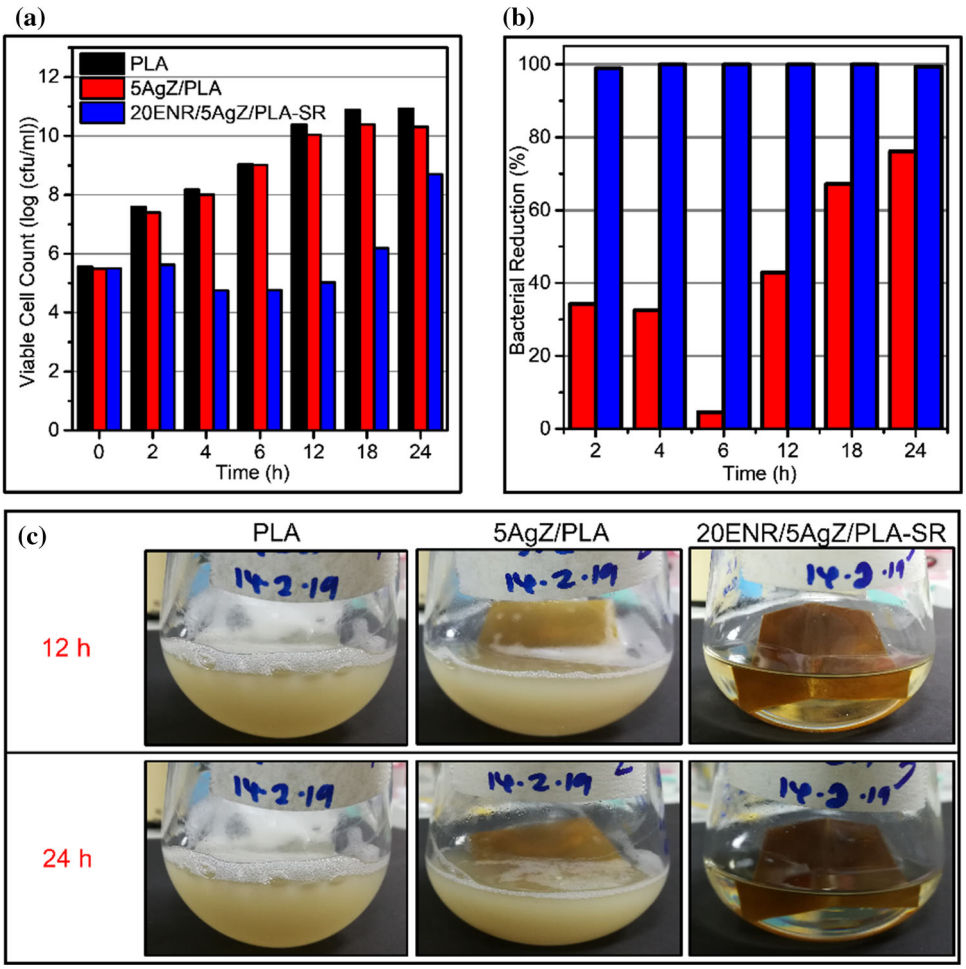

Figure 12 Antibacterial activity of PLA, 5AgZ/PLA, and 20ENR/5AgZ/PLA-SR against *S. aureus* (the bacterium was cultured in MH broth in the presence of either composites), **a** viable cell count of PLA, 5AgZ/PLA and 20ENR/5AgZ/PLA, **b** percentage of bacterial reduction as compared to PLA, and **c** broth appearance of the three culture conditions at 12 and 24 h.

(Fig. 12c). According to these results, it could be noted that ENR acted as an antibacterial promoter and significantly enhanced the antibacterial performances of the composites.

Mechanical properties of the composites

The mechanical properties of neat PLA, 5AgZ/PLA, and ENR/AgZ/PLA composites-SR were also investigated. The tensile strength, modulus, and elongation at break of the samples are itemized in Table 5. The modulus of neat PLA was equal to 2300 MPa. The incorporation of zeolites into PLA increased the modulus of the composites to 2600 MPa, which is due to the fact that the addition of rigid filler leads to the increase in the tensile modulus of the composites. This result was corresponded with the publication reported elsewhere [35]. In the case of ENR/AgZ/PLA composites, the result showed that at 10 wt% ENR, the modulus of the composites decreased to 1653 MPa. The moduli of 20ENR/5AgZ/PLA-SR and 20ENR/5AgZ/PLA-SR were 1215 MPa and 497 MPa, respectively. It could be noted that further increasing the ENR contents leads to the decrease in the modulus of the composites because of the flexible characteristic of ENR phase [24, 26].

Apart from tensile properties, the impact strength of neat PLA and the composites-SR was also compared as plotted in Fig. 13. Because of the brittle nature of PLA, the impact strength was 4.7 kJ/m^2 and the failure type was categorized as complete break in which the specimen separated into two pieces. For 5AgZ/PLA, the incorporation of zeolites into PLA matrix does not increase the impact strength (data not shown). After blending with rubber, the impact strength of the composites was increased significantly. Twofold and threefold increases in the impact strength were found in 10ENR/5AgZ/PLA-SR and 20ENR/5AgZ/PLA-SR, respectively. Besides, the breaking behavior of the

Table 5 Tensile strength, modulus, and elongation at break of neat PLA and its composites

Samples	Tensile strength (MPa)	Modulus (MPa)	Elongation at break (%)
PLA	64.0 ± 2.2	2300 ± 78	5.6 ± 0.8
5AgZ/PLA	58.0 ± 2.1	2600 ± 136	5.3 ± 0.5
10ENR/5AgZ/PLA-SR	37.6 ± 1.7	1653 ± 218	8.0 ± 2.2
20ENR/5AgZ/PLA-SR	19.1 ± 3.6	1215 ± 166	5.2 ± 0.9
30ENR/5AgZ/PLA-SR	10.0 ± 0.9	497 ± 75	7.6 ± 2.1

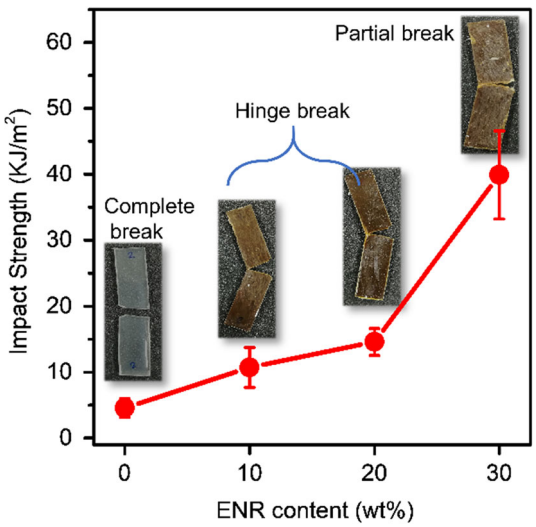

Figure 13 Plots of impact strength and physical appearance of specimens after testing of PLA and ENR/AgZ/PLA composites-SR containing different amount of ENR ranging from 10 to 30 wt%.

specimens changed from complete break to hinge break. Further increasing the content of ENR to 30 wt%, the impact strength increased by 9 times and the type of failure was categorized as partial break. The increase in toughness of the composites was attributed to the presence of rubber phase and the interaction between PLA and ENR created by the carbonyl groups and the epoxide groups [48, 49].

Conclusion

Thermoplastic composites of ENR/AgZ/PLA possessing the antibacterial properties were prepared, and this work was the first report to utilize ENR as an antibacterial promoter. Incorporating ENR into the composites increased the water absorption of composites, thus facilitating the diffusion of silver ions to the surface of the composites. In terms of preparing methodology, the roll milling process improved the homogeneity of the composites (good AgZ distribution), caused the zeolite delocalization, and also altered the morphology of the composites. Hence, the antibacterial activity of composites-SR significantly increased the antibacterial activity compared to composites-S. The antibacterial efficiency of the composites was dependent on the amounts of ENR and AgZ in the composites. The composites having 20 wt% ENR and 5 wt% AgZ were considered as the most effective composites. Moreover, the quantitative analysis showed that the composites-SR exhibited the efficient ability to inhibit the growth of bacteria and the reduction percentage of 98–99% was far better than that of AgZ/PLA composites.

In summary, not only does this work give the novel method, which is simple but effective, to prepare ENR/AgZ/PLA composites, but also widen the application of ENR for promoting the antibacterial activity of PLA composites. The knowledge given can be of benefits to developing antibacterial PLA composites.

Acknowledgements

Partial support from an ERASMUS + grant 2015-1-FR01-KA107-014841 between Mahidol University and Le Mans University is gratefully acknowledged. Teaching assistance scholarship of Faculty of Science, Mahidol University to M. Taranamai is very much appreciated.

Compliance with ethical standards

Conflicts of interest The authors declare no conflicts of interest.

References

[1] Kenawy E-R, Worley SD, Broughton R (2007) The chemistry and applications of antimicrobial polymers: a state-of-the-art review. Biomacromol 8:1359–1384. https://doi.org/10.1021/bm061150q

[2] Francolini I, Donelli G, Stoodley P (2003) Polymer designs to control biofilm growth on medical devices. Rev Environ Sci Biotechnol 2:307–319. https://doi.org/10.1023/b:Resb.0000040469.26208.83

[3] Imazato S (2003) Antibacterial properties of resin composites and dentin bonding systems. Dent Mater 19:449–457. https://doi.org/10.1016/S0109-5641(02)00102-1

[4] Markarian J (2009) Antimicrobials find new healthcare applications. Plastic Addit Compd 11:18–22. https://doi.org/10.1016/S1464-391X(09)70030-3

[5] Appendini P, Hotchkiss JH (2002) Review of antimicrobial food packaging. Innov Food Sci Emerg Technol 3:113–126. https://doi.org/10.1016/S1466-8564(02)00012-7

[6] Monteiro DR, Gorup LF, Takamiya AS, Ruvollo-Filho AC, Camargo E, Barbosa DB (2009) The growing importance of materials that prevent microbial adhesion: antimicrobial effect of medical devices containing silver. Int J Antimicrob Agents 34:103–110. https://doi.org/10.1016/j.ijantimicag.2009.01.017

[7] Khare MD, Bukhari SS, Swann A, Spiers P, McLaren I, Myers J (2007) Reduction of catheter-related colonisation by the use of a silver zeolite-impregnated central vascular catheter in adult critical care. J Infect 54:146–150. https://doi.org/10.1016/j.jinf.2006.03.002

[8] Inoue Y, Hoshino M, Takahashi H et al (2002) Bactericidal activity of Ag–zeolite mediated by reactive oxygen species under aerated conditions. J Inorg Biochem 92:37–42. https://doi.org/10.1016/S0162-0134(02)00489-0

[9] Quintavalla S, Vicini L (2002) Antimicrobial food packaging in meat industry. Meat Sci 62:373–380. https://doi.org/10.1016/S0309-1740(02)00121-3

[10] Loertzer H, Soukup J, Hamza A et al (2006) Use of catheters with the AgION antimicrobial system in kidney transplant recipients to reduce infection risk. Transplant Proc 38:707–710. https://doi.org/10.1016/j.transproceed.2006.01.064

[11] Rusin P, Bright K, Gerba C (2003) Rapid reduction of *Legionella pneumophila* on stainless steel with zeolite coatings containing silver and zinc ions. Lett Appl Microbiol 36:69–72. https://doi.org/10.1046/j.1472-765X.2003.01265.x

[12] Cowan MM, Abshire KZ, Houk SL, Evans SM (2003) Antimicrobial efficacy of a silver-zeolite matrix coating on stainless steel. J Ind Microbiol Biotechnol 30:102–106. https://doi.org/10.1007/s10295-002-0022-0

[13] Galeano B, Korff E, Nicholson WL (2003) Inactivation of vegetative cells, but not spores, of *Bacillus anthracis*, *B. cereus*, and *B. subtilis* on stainless steel surfaces coated with an antimicrobial silver- and zinc-containing zeolite formulation. Appl Environ Microbiol 69:4329–4331

[14] Casemiro LA, Martins CHG, Pires-de-Souza F, Panzeri H (2008) Antimicrobial and mechanical properties of acrylic resins with incorporated silver–zinc zeolite—part I. Gerodontology 25:187–194. https://doi.org/10.1111/j.1741-2358.2007.00198.x

[15] Abe Y, Ishii M, Takeuchi M, Ueshige M, Tanaka S, Akagawa Y (2004) Effect of saliva on an antimicrobial tissue conditioner containing silver–zeolite. J Oral Rehabil 31:568–573. https://doi.org/10.1111/j.1365-2842.2004.01267.x

[16] Hotta M, Nakajima H, Yamamoto K, Aono M (1998) Antibacterial temporary filling materials: the effect of adding various ratios of Ag–Zn–Zeolite. J Oral Rehabil 25:485–489. https://doi.org/10.1046/j.1365-2842.1998.00265.x

[17] Yeo SY, Lee HJ, Jeong SH (2003) Preparation of nanocomposite fibers for permanent antibacterial effect. J Mater Sci 38:2143–2147. https://doi.org/10.1023/a:1023767828656

[18] Silver S (2003) Bacterial silver resistance: molecular biology and uses and misuses of silver compounds. FEMS Microbiol Rev 27:341–353. https://doi.org/10.1016/S0168-6445(03)00047-0

[19] Yoshida CMP, Bastos CEN, Franco TT (2010) Modeling of potassium sorbate diffusion through chitosan films. LWT Food Sci Technol 43:584–589. https://doi.org/10.1016/j.lwt.2009.10.005

[20] Ouattara B, Simard RE, Piette G, Bégin A, Holley RA (2000) Diffusion of acetic and propionic acids from Chitosan-based antimicrobial packaging films. J Food Sci 65:768–773. https://doi.org/10.1111/j.1365-2621.2000.tb13584.x

[21] Odani H, Uchikura M, Ogino Y, Kurata M (1983) Diffusion and solution of methanol vapor in poly(2-vinylpyridine)-block- polyisoprene and poly(2-vinylpyridine)-block-polystyrene. J Membr Sci 15:193–208. https://doi.org/10.1016/S0376-7388(00)80398-1

[22] Ahmed J, Hiremath N, Jacob H (2017) Antimicrobial efficacies of essential oils/nanoparticles incorporated polylactide films against *L. monocytogenes* and *S. typhimurium* on contaminated cheese. Int J Food Prop 20:53–67. https://doi.org/10.1080/10942912.2015.1131165

[23] Fernández A, Soriano E, Hernández-Muñoz P, Gavara R (2010) Migration of antimicrobial silver from composites of polylactide with silver zeolites. J Food Sci 75:E186–E193. https://doi.org/10.1111/j.1750-3841.2010.01549.x

[24] Pongtanayut K, Thongpin C, Santawitee O (2013) The effect of rubber on morphology, thermal properties and mechanical properties of PLA/NR and PLA/ENR blends. Energy Procedia 34:888–897. https://doi.org/10.1016/j.egypro.2013.06.826

[25] Zakaria Z, Islam MS, Hassan A et al (2013) Mechanical properties and morphological characterization of PLA/Chitosan/epoxidized natural rubber composites. Adv Mater Sci Eng. https://doi.org/10.1155/2013/629092

[26] Wang Y, Chen K, Xu C, Chen Y (2015) Supertoughened biobased poly(lactic acid)–epoxidized natural rubber thermoplastic vulcanizates: fabrication, co-continuous phase structure, interfacial in situ compatibilization, and toughening mechanism. J Phys Chem B 119:12138–12146. https://doi.org/10.1021/acs.jpcb.5b06244

[27] Jaratrotkamjorn R, Khaokong C, Tanrattanakul V (2012) Toughness enhancement of poly(lactic acid) by melt blending with natural rubber. J Appl Polym Sci 124:5027–5036. https://doi.org/10.1002/app.35617

[28] Tham WL, Poh BT, Mohd Ishak ZA, Chow WS (2016) Epoxidized natural rubber toughened poly(lactic acid)/halloysite nanocomposites with high activation energy of water diffusion. J Appl Polym Sci. https://doi.org/10.1002/app.42850

[29] Shameli K, Ahmad MB, Zargar M, Yunus WMZW, Ibrahim NA (2011) Fabrication of silver nanoparticles doped in the zeolite framework and antibacterial activity. Int J Nanomed 6:331–341. https://doi.org/10.2147/IJN.S16964

[30] Phinyocheep P, Phetphaisit CW, Derouet D, Campistron I, Brosse JC (2005) Chemical degradation of epoxidized natural rubber using periodic acid: preparation of epoxidized liquid natural rubber. J Appl Polym Sci 95:6–15. https://doi.org/10.1002/app.20812

[31] Bradbury JH, Perera MCS (1985) Epoxidation of natural rubber studied by nmr spectroscopy. J Appl Polym Sci 30:3347–3364. https://doi.org/10.1002/app.1985.070300817

[32] Davey JE, Loadman MJR (1984) A chemical demonstration of the randomness of epoxidation of natural rubber. Brit Polym J 16:134–138. https://doi.org/10.1002/pi.4980160305

[33] Burfield DR, Lim K-L, Law K-S, Ng S (1984) Analysis of epoxidized natural rubber. A comparative study of d.s.c., n.m.r., elemental analysis and direct titration methods. Polymer 25:995–998. https://doi.org/10.1016/0032-3861(84)90086-7

[34] Kourki H, Famili MHN, Mortezaei M, Malekipirbazari M (2018) Mixing challenges for SiO_2/polystyrene nanocomposites. J Thermoplast Compos 31:709–726. https://doi.org/10.1177/0892705717718599

[35] Yuzay IE, Auras R, Selke S (2010) Poly(lactic acid) and zeolite composites prepared by melt processing: morphological and physical–mechanical properties. J Appl Polym Sci 115:2262–2270. https://doi.org/10.1002/app.31322

[36] Wang H, Sun X, Seib P (2001) Strengthening blends of poly(lactic acid) and starch with methylenediphenyl diisocyanate. J Appl Polym Sci 82:1761–1767. https://doi.org/10.1002/app.2018

[37] Shogren R (1997) Water vapor permeability of biodegradable polymers. J Environ Polym Degrad 5:91–95. https://doi.org/10.1007/bf02763592

[38] Mat Uzir Wahit AH, Ibrahim AN, Zawawi NA, Kunasegeran K (2015) Mechanical, thremal, and chemical resistance of epoxidized natural rubber toughened polylactic acid blends. Sains Malays 44:1615–1623

[39] Spriger G, Shen C (1976) Moisture absorption and desorption of composite materials. J Compos Mater 20:2–20

[40] Kushwaha PK, Kumar R (2009) Studies on water absorption of bamboo-polyester composites: effect of silane treatment of mercerized bamboo. Polym Plast Technol Eng 49:45–52. https://doi.org/10.1080/03602550903283026

[41] Pötschke P, Krause B, Buschhorn ST et al (2013) Improvement of carbon nanotube dispersion in thermoplastic composites using a three roll mill at elevated temperatures. Compos Sci Technol 74:78–84. https://doi.org/10.1016/j.compscitech.2012.10.010

[42] Jo Y, Garcia CV, Ko S et al (2018) Characterization and antibacterial properties of nanosilver-applied polyethylene and polypropylene composite films for food packaging applications. Food Biosci 23:83–90. https://doi.org/10.1016/j.fbio.2018.03.008

[43] Kim JS, Kuk E, Yu KN et al (2007) Antimicrobial effects of silver nanoparticles. Nanomedicine 3:95–101. https://doi.org/10.1016/j.nano.2006.12.001

[44] Jokar M, Abdul Rahman R, Ibrahim NA, Abdullah LC, Tan CP (2012) Melt production and antimicrobial efficiency of low-density polyethylene (LDPE)-silver nanocomposite film. Food Bioprocess Tech 5:719–728. https://doi.org/10.1007/s11947-010-0329-1

[45] Cho K-H, Park J-E, Osaka T, Park S-G (2005) The study of antimicrobial activity and preservative effects of nanosilver ingredient. Electrochim Acta 51:956–960. https://doi.org/10.1016/j.electacta.2005.04.071

[46] Becaro AA, Puti FC, Correa DS, Paris EC, Marconcini JM, Ferreira MD (2015) Polyethylene films containing silver nanoparticles for applications in food packaging: characterization of physico-chemical and anti-microbial properties. J Nanosci Nanotechnol 15:2148–2156. https://doi.org/10.1166/jnn.2015.9721

[47] Prapruddivongs C, Sombatsompop N (2012) Roles and evidence of wood flour as an antibacterial promoter for triclosan-filled poly(lactic acid). Compos B 43:2730–2737. https://doi.org/10.1016/j.compositesb.2012.04.032

[48] Zhang C, Wang W, Huang Y et al (2013) Thermal, mechanical and rheological properties of polylactide

toughened by expoxidized natural rubber. Mater Des 45:198–205. https://doi.org/10.1016/j.matdes.2012.09.024

[49] Nematollahi M, Jalali-Arani A, Modarress H (2019) High-performance bio-based poly(lactic acid)/natural rubber/epoxidized natural rubber blends: effect of epoxidized natural rubber on microstructure, toughness and static and dynamic mechanical properties. Polym Int 68:439–446. https://doi.org/10.1002/pi.5727

Publisher's Note Springer Nature remains neutral with regard to jurisdictional claims in published maps and institutional affiliations.